doi:10.3772/j.issn.1006-6748.2019.01.003

Experimental study on vibration suppression of gear shaft misalignment with ISFD①

Lu Kaihua (路凯华), He Lidong②, Zhang Yipeng, Chen Zhao, Yan Wei
(Beijing Key Laboratory of Health Monitoring and Self-Recovery for High-End Mechanical Equipment, Beijing University of Chemical Technology, Beijing 100029, P. R. China)

Abstract

Misalignment faults in gear systems lead to violent vibration and noise, shortening the life of equipment. The aim of this work is the demonstration of vibration suppression of parallel-misaligned gear shafts using an integral squeeze film damper (ISFD). Using a first grade spur gear in engineering for reference, an open first-grade spur gear system is built and the vibration characteristics of the gear system with rigid supports and ISFD elastic damping supports are studied under different degrees of misalignment. The experimental results show that ISFD supports have excellent damping and vibration attenuation characteristics, which have improved control of the gear system vibration in horizontal, vertical and axial directions under different degrees of misalignment. This work shows that an ISFD structure can effectively suppress vibration of characteristic frequency components and resonance modulation frequency components. The test results provide evidence for the application of ISFD in vibration control of gear shaft misalignment faults in engineering.

Key words: gear shaft, parallel misalignment, integral squeeze film damper (ISFD), vibration suppression

0 Introduction

Shaft misalignment is one of the main forms of faults of rotating machineries, and accounts for more than 60% of rotor system faults. Rotor misalignment refers to the scenario where the axes of two adjacent rotors are not in line. This results in additional bending moment and torsional moment in the rotor system, and subsequently leads to a series of vibrations, which can damage the equipment when the situation is serious[1]. The reasons for misalignment include design and manufacturing errors, installation errors, and operating factors. Some forms of misalignment can be easily corrected. For instance, if the misalignment is caused by uneven quality of components, measurement errors, machining accuracy error, differences in bolt tightness, foundation subsidence, or coupling dislocation caused by uneven heating in the process of mechanical assembly, the misalignment can usually be readjusted when the machine is not running. However, misalignments caused by various kinds of complex scenarios in the operating process are related to the operation of the machine, and therefore are difficult to be eliminated. Many scholars have studied rotating machinery by focusing on the causes of misalignment[2], dynamic characteristics[3] and the influence of misalignment on the stability of shafting[4,5]. However, most of the work is aimed at the diagnosis and analysis of misalignment faults. The existing research regarding rotor misalignment is primarily focused on the rotor coupling bearing system. Actual machinery usually contains several gear systems, such as reducers, transmission, engine power transmission devices, and so on. As an important part of the engine transmission system, the gear assembly operates with a large transmission power and complex structural features because of its special purpose[6]. The misalignment of the gear system occurs mainly in the couplings between the gear system and other components[7]. Gear shaft misalignment causes tooth profile error of a distributed type, which results in vibration and noise of the gear system. Online vibration control methods of gear system misalignment have been seldom studied. In engineering, parallel misalignment is common when there is an improper installation of the gearbox[8]. This paper mainly discusses the parallel

① Supported by the National Basic Research Program of China (No. 2012CB026000), 2015 Beijing Scientific Research and Graduate Training Project (No. 0318-21510028008) and Key Laboratory Fund for Ship Vibration and Noise (No. 614220406020717).

② To whom correspondence should be addressed. E-mail: 1963he@163.com

Received on May 8, 2018

misalignment of gear shafts.

Reduction of rotor vibration is very important for safe and efficient functioning of these rotating machines. Applying damping to rotor supports is a popular technique for vibration reduction[9]. Squeeze film dampers (SFD) have been used for decades in both aerospace and ground based turbomachinery[10-12]. The improved integral squeeze film damper (ISFD) provides viscous damping to rotating structures, allowing the reduction of rotor-bearing lateral vibration amplitudes and providing safe isolation to other structural components[13]. The specific structure of ISFD has allowed many problems with traditional squeeze film dampers to be resolved[14]. Problems such as nonlinear oil film, complex structure, large occupation space, difficult assembly, high-accumulated error and nonlinear change of the stiffness and damping characteristics can be solved. ISFD has been applied in many rotating machines such as compressors, turbines, and engines, for the purpose of reducing vibration of the rotor at critical speeds and improving stability of the rotor system[15].

The present work examines the effect of ISFD on vibration suppression of rotor misalignment faults, and illustrates that ISFD can effectively reduce the vibration caused by misalignment faults[16]. In addition, the vibration control law of gear shafts with ISFD and its installation position is studied. It is shown that ISFD elastic damping support can suppress impact vibration due to gear meshing and has excellent damping and vibration reduction characteristics[17,18]. Parallel misalignment faults usually occur in gearboxes when the installation is improper, and can cause severe noise and vibration, resulting in equipment damage.

In this paper, the effect of ISFD on the suppression of vibrations caused by parallel-misaligned gear shafts is studied. Four sets of experimental ISFD elastic damping support structures have been designed and manufactured. Taking the first-grade spur gear transmission in engineering as reference, an open first-grade spur gear system has been set up to result in misalignment fault. By comparing the vibrations of the gear shaft equipped with rigid support and ISFD elastic damping support, the effectiveness of ISFD for suppressing the misalignment vibration of gear shafts is studied.

1 Integral squeeze film damper

1.1 Structural features of ISFD

ISFD is a bearing damper, made via wire cutting manufacturing, rendering its structure simple and compact. The most important feature is that it has the ability to function as bearing support, but also provide damping for the rotor system. The ISFD designed for experiments used in this work is shown in Fig. 1. Table 1 gives the basic structural parameters of the damper. The structure consists of an outer rim and inner rim. The outer rim and inner rim are connected by a fixed number of S-shaped spring structures. S-shaped springs allow pressure to be distributed evenly and can absorb shock load effectively. The radial static stiffness of the bearing support system is determined by these S-shaped elastic structures. Between the inner and outer rim is the gap, which serves as the main squeeze film area. The gap is 0.2 mm wide and the fluid is squeezed in this gap, thereby providing damping required by the system.

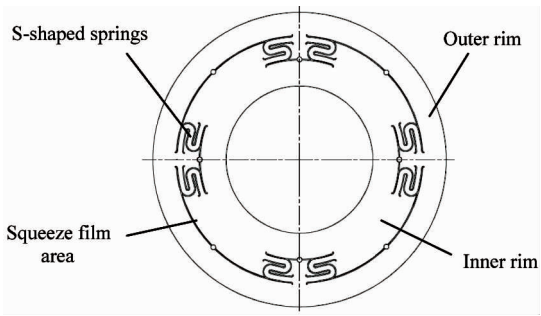

Fig. 1 ISFD designed for experiments

Table 1 Basic structural parameters of ISFD

Item	Value
Axial length (mm)	10
Radial height (mm)	20.3
Radial thickness (mm)	4.9
Oil film clearance (mm)	0.2
Distribution angle of S-shaped spring (°)	52
Inner diameter (mm)	30
Outer diameter (mm)	60

1.2 Working mechanism

The rotor system under different working conditions has its own optimal damping and stiffness values. Stiffness and damping in the new ISFD structure are relatively independent, such that stiffness and damping in the support system don't have a direct relationship. Therefore, the stiffness and damping of the structure are decoupled.

The S-shaped springs in the ISFD are the only major contributors to the radial bearing support stiffness[15]. Fig. 2 shows the displacement clouds of ISFD under a loading of 2 000 N. By changing the structural size of the S-shaped springs, a specific radial stiffness can be obtained. This allows for good predictability and

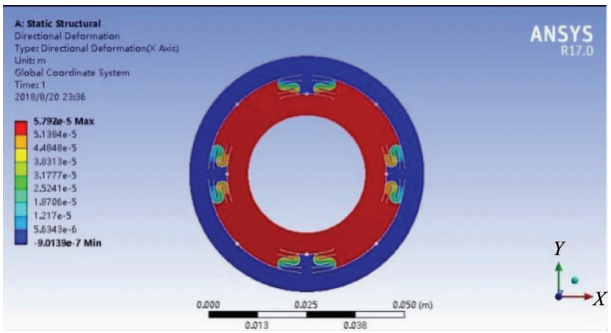

(a) X direction

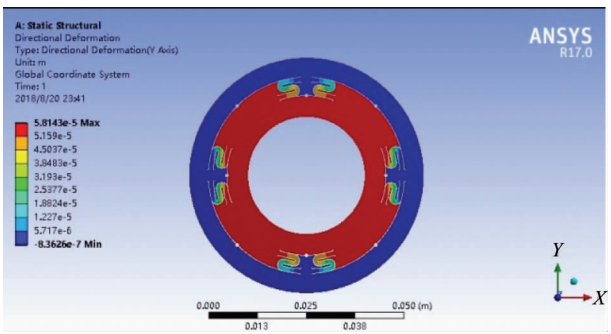

(b) Y direction

Fig. 2 Displacement clouds of ISFD under a loading of 2000 N

precise placement of critical speeds and rotor modes.

The energy dissipation mechanism of the conventional squeeze film damper (SFD) is based on generating fluid pressure Δp by squeezing the oil film. This increased pressure promotes movement of lubricating oil along the circumference. Flow friction due to circumferential motion (ΔQs) of the fluid produces damping that dissipates the vibration energy. There is obviously significant non-linearity as a result of this approach. Compared to SFD, the energy dissipation mechanism of the ISFD is unique. Fig. 3 shows the flow model comparison between a conventional SFD and an ISFD[15]. Unlike the conventional SFD 2π oil film, the circumferentially distributed S-shaped springs of ISFD divide the circumferential flow of the oil film into several local regions. As well, they do not allow circumferential flow of the fluid ($\Delta Qs = 0$), which provides a different fluid flow boundary condition. The squeeze film effect of each compartment and the piston effect of the S-springs are used to provide damping for the rotor system and eliminate the generation and influence of nonlinearity over a wide range.

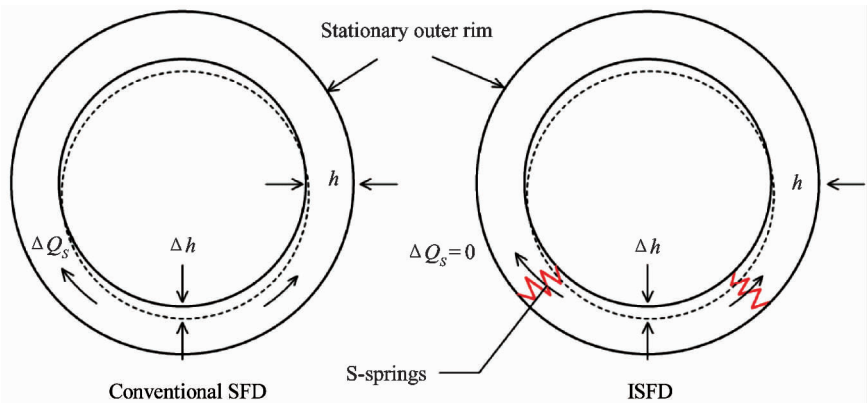

Fig. 3 Damping mechanism: conventional SFD versus ISFD

Fig. 4 shows mechanical models of a traditional bearing support system and an ISFD bearing support system. By comparing with the two models, it can be seen that the stiffness of the ISFD structure is several orders of magnitude lower than that of the bearing. In this way, vibrational deformation during transmission is mainly concentrated on the elastic support, which can absorb the vibration energy. In addition, the oil film damping provided by ISFD can dissipate vibration energy[19]. As a result, an ISFD can provide relatively low stiffness through the S-type structure while providing greater damping in the squeeze film damper, effectively increasing damping ratio of the system[20].

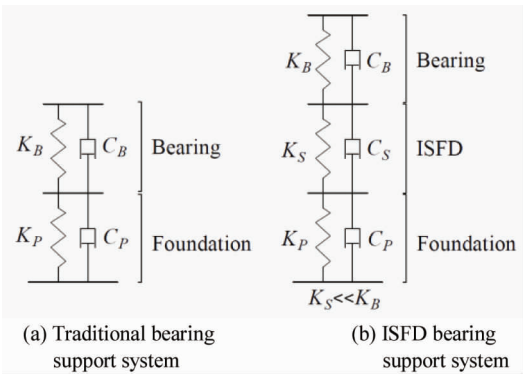

Fig. 4 Mechanical models of traditional bearing support system and the ISFD bearing support system

2 Dynamic model of parallel-misaligned rotor with ISFD

In analyzing the ISFD vibration damping mechanism, the bearing-rotor-ISFD can be transformed into the model shown in Fig. 5. The ISFD designed for this study is concentric. It is assumed that the static equilibrium point of the integral squeeze film damper coincides with the rotor center. For convenience, the rotor system is assumed to be a continuous system and, consequently, the concentrated mass method is utilized to solve the equation of motion.

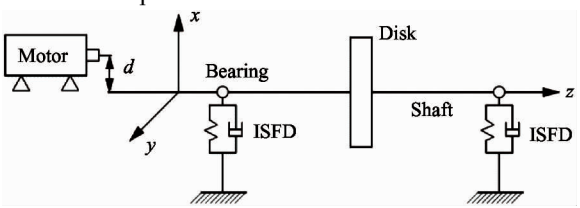

Fig. 5 Dynamic model of parallel-misaligned rotor with ISFD

As shown in Fig. 5, when there is a parallel misalignment in the axis, the radial alternating force acting on the shaft is Fr:

$$F_r = K \cdot d(1 + \cos 2\omega t)/4 \tag{1}$$

where, d stands for the eccentricity of the two axes, K is the radial stiffness of the coupling, ω is the speed of the shaft.

For the rotor disk, the equation of motion is

$$\begin{cases} m\ddot{x}_m = k(x_0 - x_m) + F_{qx} \\ m\ddot{y}_m = k(y_0 - y_m) + F_{qy} \end{cases} \tag{2}$$

For the shaft, the equation of motion is

$$\begin{cases} m_0\ddot{x}_0 = k(x_m - x_0) - \Delta f_{1x} - F_{rx} \\ m_0\ddot{y}_0 = k(y_m - y_0) - \Delta f_{1y} - F_{ry} \end{cases} \tag{3}$$

For the bearings, the equation of motion is

$$\begin{cases} m_s\ddot{x}_s = \Delta f_{1x} - k_w x_s - \Delta f_{2x} \\ m_s\ddot{y}_s = \Delta f_{1y} - k_w y_s - \Delta f_{2y} \end{cases} \tag{4}$$

The bearing force increment can be expressed as

$$\begin{cases} \Delta f_{1x} = k_{xx}(x_0 - x_s) + k_{xy}(y_0 - y_s) \\ \qquad + c_{xx}(\dot{x}_0 - \dot{x}_s) + c_{xy}(\dot{y}_0 - \dot{y}_s) \\ \Delta f_{1y} = k_{yx}(x_0 - x_s) + k_{yy}(y_0 - y_s) \\ \qquad + c_{yx}(\dot{x}_0 - \dot{x}_s) + c_{yy}(\dot{y}_0 - \dot{y}_s) \end{cases} \tag{5}$$

The squeeze film damping oil film force increment can be expressed as

$$\begin{cases} \Delta f_{2x} = k_{xxf}x_s + k_{xyf}x_s + c_{xxf}\dot{x}_s + c_{xyf}\dot{y}_s \\ \Delta f_{2y} = k_{yxf}x_s + k_{yyf}x_s + c_{yxf}\dot{x}_s + c_{yyf}\dot{y}_s \end{cases} \tag{6}$$

where, m stands for the mass of the disk; x_m and y_m are the displacement of the disk in the x and y directions, respectively; m_o stands for the mass of the rotor; x_o and y_o are the displacements of the rotor in the x and y directions, respectively; m_s is the bearing quality; x_s and y_s are the displacement of the bearing in the x and y directions, respectively; k is the stiffness of the rotor; k_w represents the stiffness of the elastic support; Δf_{1x} and Δf_{1y} are the bearing force increment in the x and y direction of the component; Δf_{2x} and Δf_{2y} are the damping oil film incremental force in the x and y direction components; c and c_f are the damping of the oil film and the damping of the squeeze oil film, respectively; F_q is the unbalanced force.

In the above equations, the eight dynamic coefficients of the oil film damper are replaced with the instantaneous oil film coefficient, and Eq. (4) – Eq. (6) are substituted into Eq. (2) and Eq. (3) to find the solution of rotor displacement using Runge-Kutta integration.

When using the rigid support structure, equations of motion of the system without squeezing oil film damping are given:

$$\begin{cases} m\ddot{x}_m = k(x_0 - x_m) + F_{qx} \\ m\ddot{y}_m = k(y_0 - y_m) + F_{qy} \\ m_0\ddot{x}_0 = k(x_m - x_0) - \Delta F_x \\ m_0\ddot{y}_0 = k(y_m - y_0) - \Delta F_y \end{cases} \tag{7}$$

Using the above equations, the response of the rotor is calculated for two cases: with ISFD and without ISFD. It can be determined by theoretical calculation that the amplitude of the misaligned rotor is greatly reduced after using ISFD.

3 Introduction of experimental devices

3.1 Support structure

To investigate the vibration reduction characteristics of gear shafts with ISFD under parallel misalignment conditions, two supporting structures are designed according to the test bench: rigid support and ISFD elastic damping support, as shown in Fig. 6. The rigid support structure consists of a bearing block, a sleeve and a rolling bearing. The elastic damping support structure consists of a bearing block, an ISFD, a rolling bearing, and sealed end covers. Fig. 6(c) is the ISFD support without sealed end covers and Fig. 6(d) is a sealed end cover composed of sealing cap and O-type rubber rings. The outer race of the ISFD is a transition fit with the bearing block. The inner race of the ISFD has an interference fit with the outer race of the ball bearing. The vibration amplitudes of the two types of supported gear systems under different degrees of parallel misalignment are examined. Results can be used to illustrate the vibration reduction characteristics of gear shafts with ISFD under different degrees of parallel misalignment.

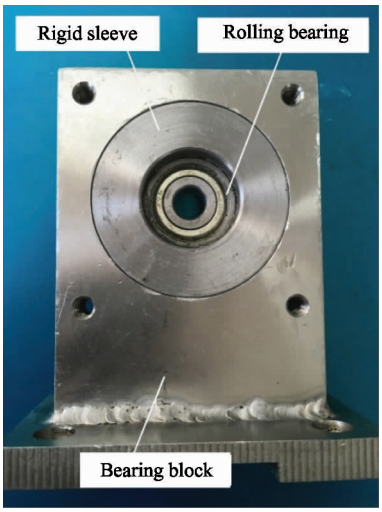

(a) Rigid support

(b) ISFD elastic damping support

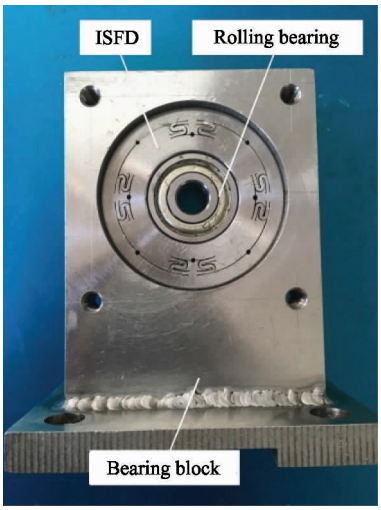

(c) ISFD without sealed end covers

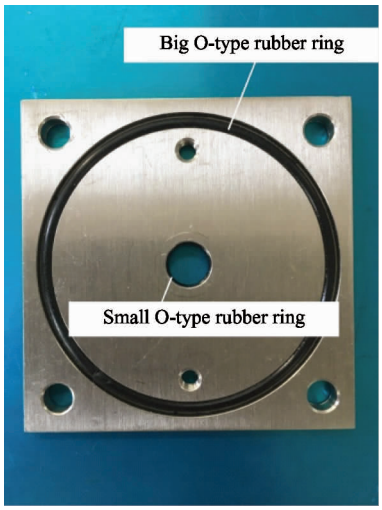

(d) Sealed end cover with O-type rubber rings

Fig. 6 Two kinds of experimental support structures

3.2 Test rig description

The test rig for the gear system is a first-grade spur gear system and is shown in Fig. 7. After determining the transmission ratio, the standard parts such as gears and bearings are selected to determine the exact meshing position of the gear. The main parameters of the gear system are listed in Table 2. The diameter of the two shafts is 10 mm. The drive and driven shaft spans are 400 mm and 180 mm respectively. The drive shaft is driven by a permanent magnet DC servomotor. By adjusting the speed controller, the output speed can be controlled in the range of 0 – 10 000 r/min. The components of test rig are secured to the base plate with bolts. The gear pair is lubricated using the drip method during the experiments.

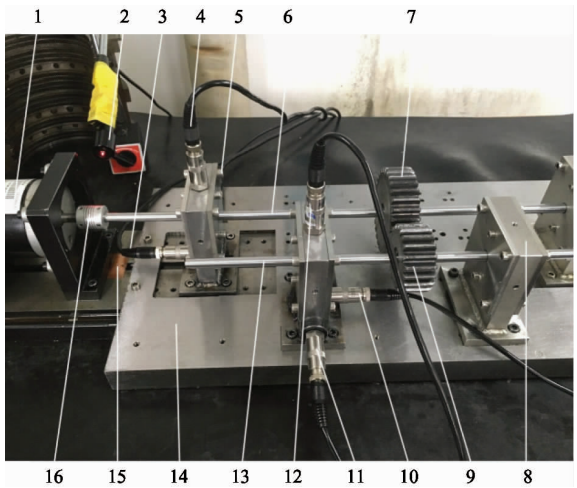

1 — Motor; 2 — Photoelectric sensors; 3 — Acceleration sensor 1; 4 — Acceleration sensor 2; 5 — Acceleration sensor 3; 6 — Drive shaft; 7 — Drive gear; 8 — ISFD elastic damping support; 9 — Driven gear; 10 — Acceleration sensor 4; 11 — Acceleration sensor 5; 12 — Acceleration sensor 6; 13 — Driven shaft; 14 — Base plate; 15 — Copper sheet; 16 — Coupling

Fig. 7 Test rig of gear system

Table 2 Parameters of the gear pair

Gear parameters	Value
Number of tooth of the drive gear	30
Number of tooth of the driven gear	20
Gear ratio	2/3
Gear modulus(mm)	3
Pressure angle(°)	20
Tooth thickness of the driven gear(mm)	30
Tooth thickness of the drive gear(mm)	28
Theoretical center distance(mm)	75

3.3 Data acquisition setting

During the experiment, the LC-8008 vibration monitoring and diagnosis system is used. This system includes 8 input channels, which can collect, store and analyze vibration in time and frequency domains along with other real-time data during operation of the gear system.

The vibration caused by shaft misalignment is mainly observed on the bearing block, and therefore the vibration signal should be measured on the bearing block[21]. Fig. 8 shows the spatial distribution of the sensors. Six acceleration sensors attached to the drive and driven bearing blocks are used to collect the vibration signal. The horizontal, vertical and axial vibrations of the drive and driven bearing blocks are all measured. Photoelectric sensors are used to measure the rotating speed.

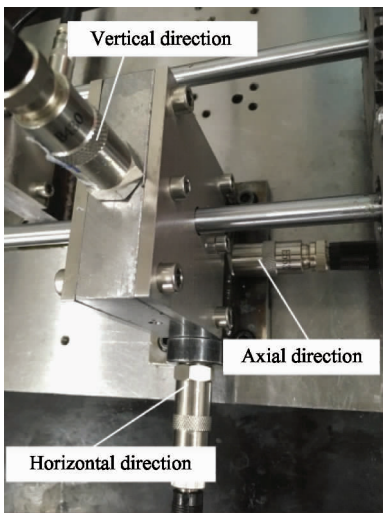

Fig. 8 Distribution of sensors

3.4 Fault setting

Gear shaft misalignment mainly occurs in coupling. As is shown in Fig. 9, the drive motor is tightened to the base plate with 2 bolts on each side of the motor. To simulate misalignment, 0.2 mm copper is added to both sides of the motor to set the parallel misalignment fault. The degree of misalignment is directly related to the amount of copper. When more copper is added, the greater is the misalignment.

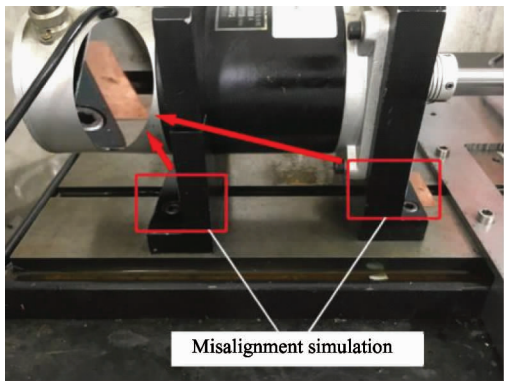

Fig. 9 Misalignment simulation

4 Results and discussion

Frequency is determined as 2 kHz with a total number of 1 024 sampling points being analyzed using the data acquisition system LC-8008. The rotating speed of the drive shaft is measured as $n_1 = 1200$ r/min by adjusting the speed controller. Next, a rotating speed of the driven shaft is determined to be $n_2 = n_1/i = 1800$ r/min. There is a certain level of speed fluctuation (± 5 r/min) presented in the experiment.

4.1 Vibration control analysis under different degrees of misalignment

By changing the number of copper sheets, the misalignment is set at 0.2 mm, 0.4 mm and 0.6 mm. Vibrations of bearing blocks are collected for gear shafts installed with a rigid support and an ISFD elastic damping support. Fig. 10 and Fig. 11 show the peak acceleration of the horizontal, vertical and axial measurement points on the drive and driven shafts under different degrees of misalignment, respectively. The results for the shafts with rigid support and ISFD support are both shown.

As seen from the experimental results shown in Fig. 10 and Fig. 11, the level of vibration of each of the measuring points reduces when the support is changed from the rigid support to the ISFD elastic damping support. Under different degrees of misalignment, the maximum amplitude of vibration reduction for the drive and driven shafts in the horizontal direction is 33.6% and 43.5%, respectively. In the vertical direction the reductions are 46.7% and 43.3% for the drive and driven shafts, respectively. Finally, in the axial direction the observed reductions in vibration are 35.9% and 42.8% for the drive and driven shafts, respectively.

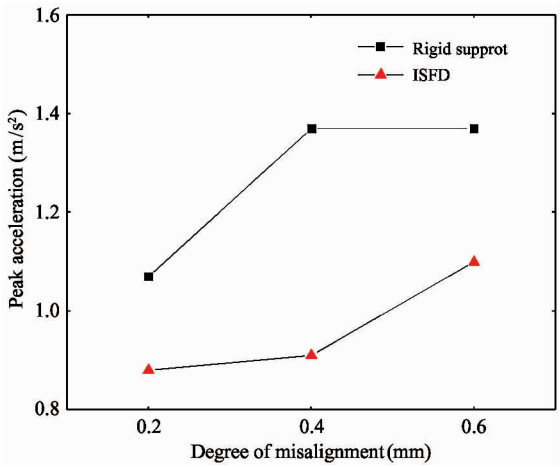

(a) Horizontal measuring point

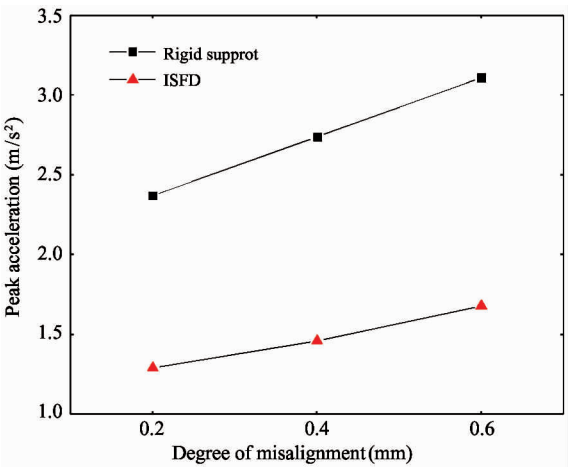

(b) Vertical measuring point

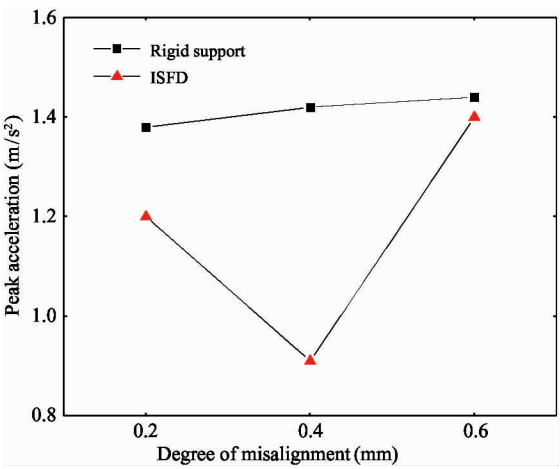

(c) Axial measuring point

Fig. 10 Comparison of vibration of drive shaft measuring points

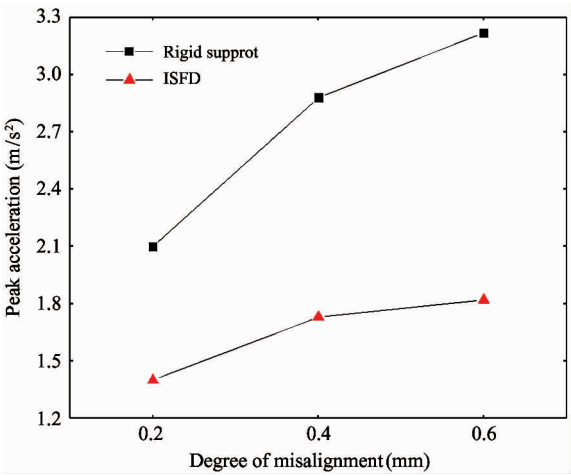

(a) Horizontal measuring point

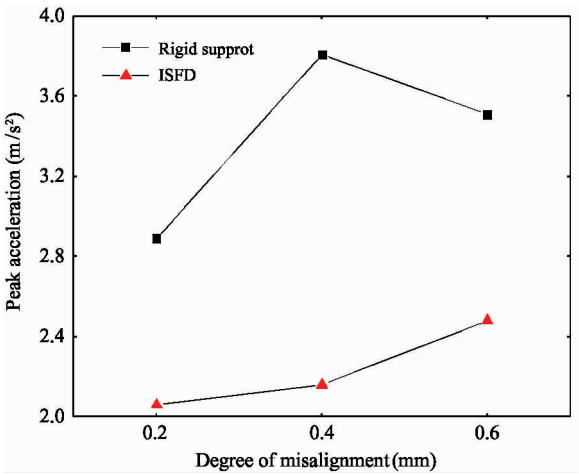

(b) Vertical measuring point

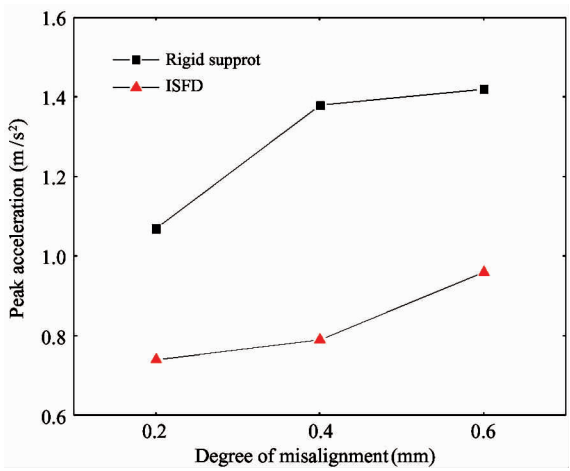

(c) Axial measuring point

Fig. 11 Comparison of vibration of driven shaft measuring points

4.2 Vibration control analysis of characteristic frequency components under parallel misalignment

To further understand the effectiveness of ISFD for suppressing misalignment vibrations of gear shafts, time domain and frequency spectra for the vibrational acceleration of each measuring point with a misalignment of 0.4 mm is analyzed and presented.

First, the time domain waveform of each measur-

ing point is analyzed. According to the sampling theorem, the sampling period of the LC-8008 is $t = \frac{1024}{2.56 \times 2000} = 0.2$ s. In order to prove the effectiveness of the ISFD in suppressing the misalignment vibration, three groups of sampling period data were selected for analysis at each measuring point. Because of the similarity of the waveform, comparisons of time domain waveforms of the horizontal measuring points of the gear shafts under the two supports are shown in Fig. 12 and Fig. 13 due to space limitations.

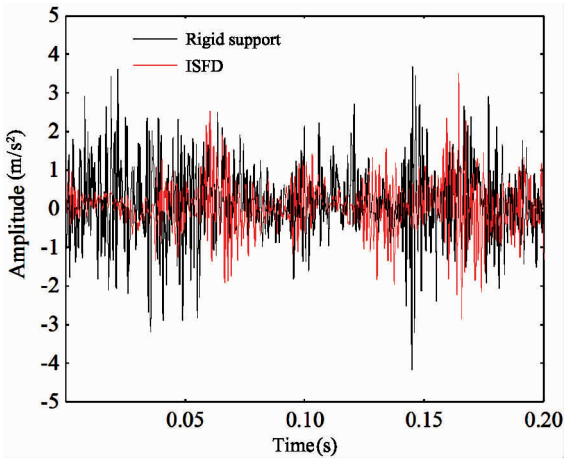

(a) The first sampling period

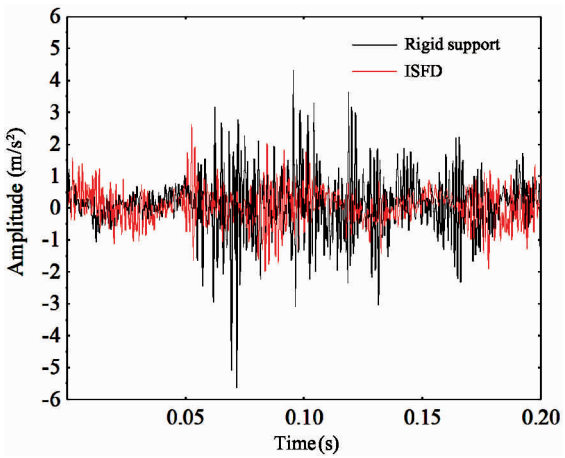

(b) The second sampling period

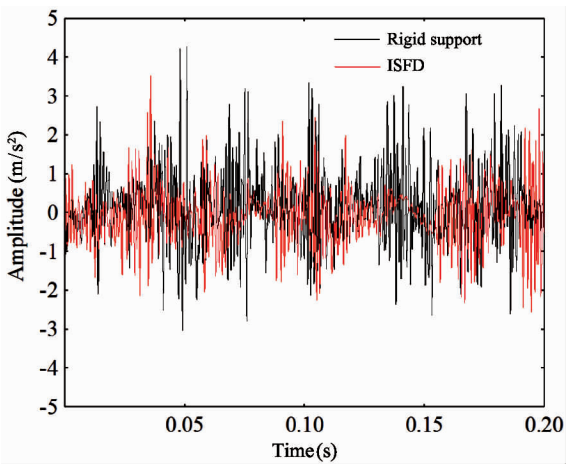

(c) The third sampling period

Fig. 12 Comparison of time domain waveform of drive shaft horizontal measuring point

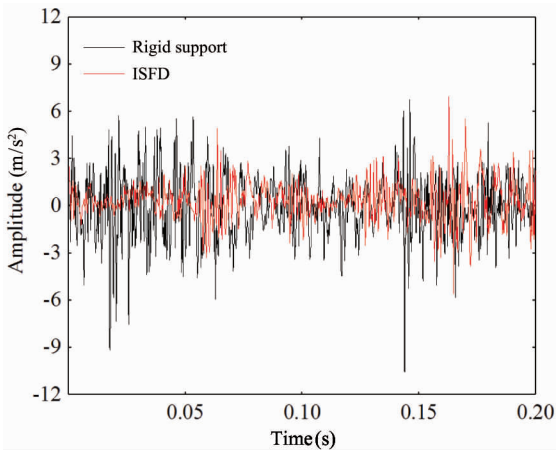

(a) The first sampling period

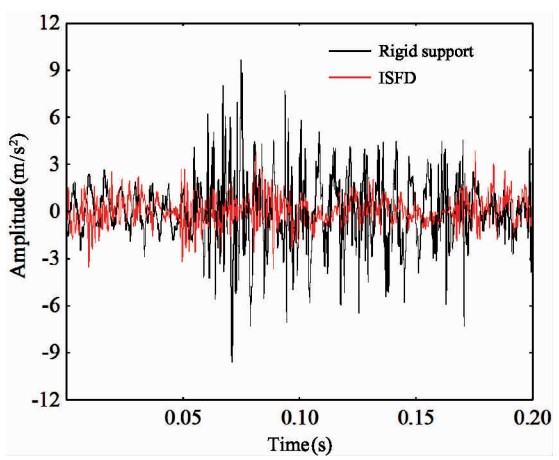

(b) The second sampling period

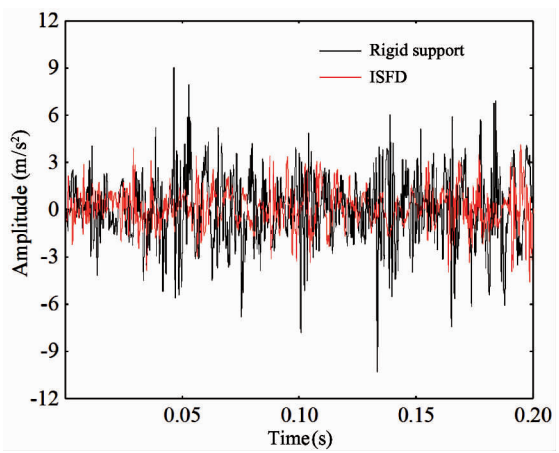

(c) The third sampling period

Fig. 13 Comparison of time domain waveform of driven shaft horizontal measuring point

From Figs12 to 13, it can be seen that shaft misalignment changes the meshing condition of the gear, resulting in an obvious impact vibration in the gear meshing transmission process. Comparing the rigid support and the ISFD support cases, it can be seen clearly from the diagram that the impact vibration has been reduced.

Next, the frequency spectrum of the measuring point is analyzed. Fig. 14 shows the comparison of frequency spectra of the horizontal, vertical and axial measuring points of the drive shaft under the two supports.

The following observations can be made from the frequency spectra above:

(1) The observed vibration frequency shows that the carrier frequency is gear meshing frequency and the modulation frequency is the rotational frequency of the fault gear shaft.

(2) Since the acceleration signal of the bearing block is measured, multiple frequency components exist in the spectra. The characteristic frequency components of the rotating frequency X, second harmonic frequency $2X$ and meshing frequency X_1 appear in the results. From the transmission parameters, it is known that the rotating frequency is $X = 20$ Hz, and the meshing frequency of the gear pair is $X_1 = 600$ Hz. The meshing frequency X_1 in the frequency spectrum has a noticeable offset relative to 600 Hz. This is likely because of the fluctuation of the motor speed during the experiment. Relatively large vibration values can be observed in the vicinity of 150 Hz, 350 Hz and 1370 Hz. This may be due to the fact that the natural frequencies of some components are excited by external conditions.

(3) It can be concluded that the vibration at the frequency components with relatively large vibration amplitude are significantly attenuated when the support is changed from rigid support to ISFD elastic damping support.

(4) High vibration at the rotating frequency X, second harmonic frequency $2X$, and meshing frequency X_1 of the horizontal and vertical measuring points are clear, as shown in Fig. 14(a) and Fig. 14(b). The vibration at the rotating frequency X and meshing frequency X_1 of the axial measuring point are noticeable, whereas the second harmonic frequency $2X$ is not obvious, as shown in Fig. 14(c). Due to the coupling of the shafts, the characteristic frequency components of the driven shaft are the same as the measuring points of the drive shaft.

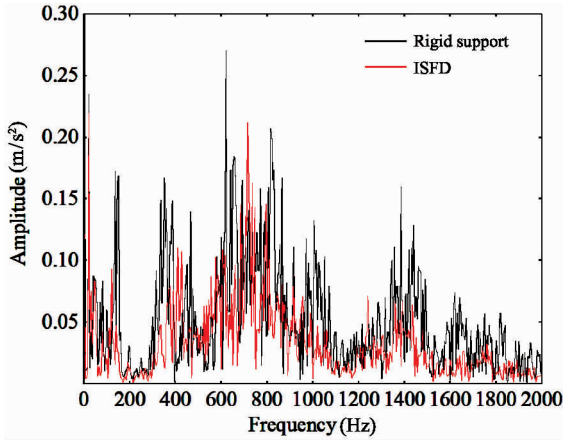

(a) Horizontal measuring point

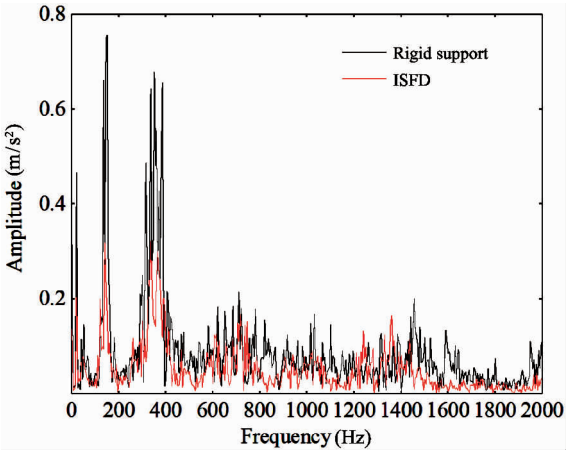

(b) Vertical measuring point

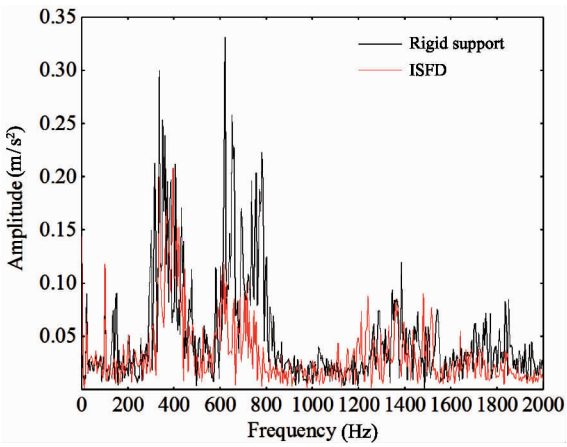

(c) Axial measuring point

Fig. 14 Comparison of frequency spectra of drive shaft measuring points

As the misalignment fault is set between the motor and the base plate, this paper mainly analyzes the characteristic frequency components of measuring points of the drive shaft, and studies the suppression

effect of the ISFD elastic damping support on the vibration control of characteristic frequency components under misalignment. To carry out an unambiguous comparison, Fig. 15 shows the spectra of the drive shaft over the range of 0 – 700 Hz for each measuring point. In addition, Tables 3 – 5 show the vibration values of the characteristic frequency components of the measuring points.

It can be seen that the vibration at the characteristic frequency components under misalignment is significantly reduced when the gear system utilizes the ISFD support compared to a rigid support. In particular, the meshing frequency component is decreased by over 70%, and resonance modulation of the gear shaft is obviously improved.

5 Conclusions

ISFD support has excellent damping vibration attenuation characteristics, which can suppress the vibration caused by parallel misalignment faults in gear systems effectively.

(1) ISFD support can reduce the vibration of gear shafts under different degrees of misalignment.

(2) ISFD has better control of gear system vibration compared to rigid supports in the horizontal, vertical and axial directions under different degrees of misalignment.

(3) Complex frequency components appear in the vibration of gear systems with misalignment fault, including characteristic frequency components and resonance modulation frequency components. It has been shown that ISFD can suppress vibration at these frequencies effectively.

(4) ISFD has the advantages of a simple structure, small occupation space, simple assembly, excellent damping performance, and great engineering application value. The test results given here provide a reference for the application of ISFD in vibration control of gear shaft misalignment faults in engineering.

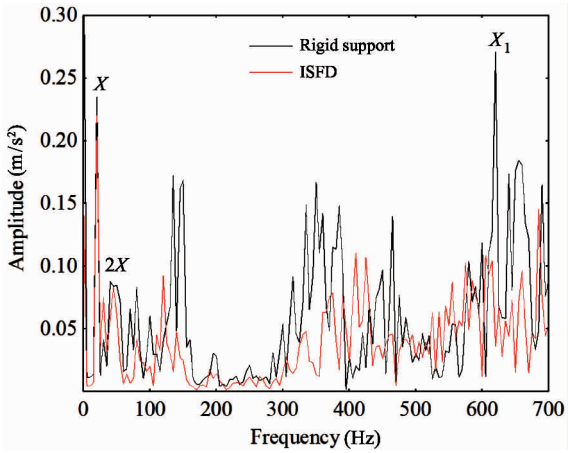

(a) Horizontal measuring point

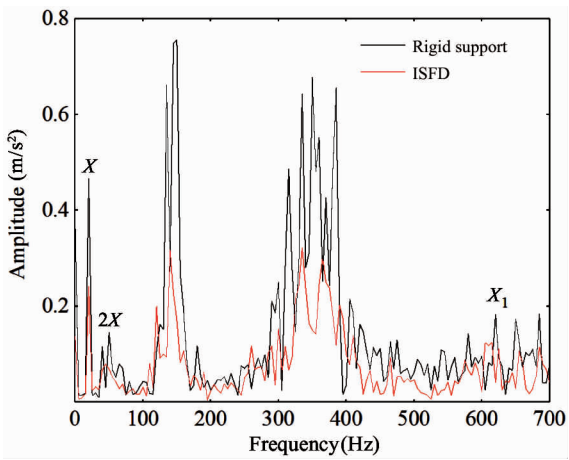

(b) Vertical measuring point

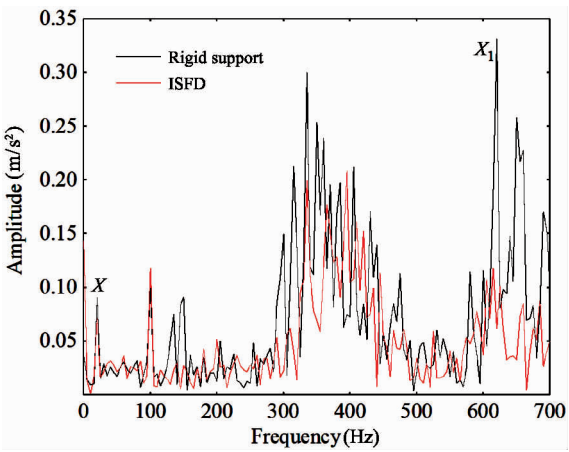

(c) Axial measuring point

Fig. 15 Comparison of data in the range of 0 – 700 Hz

Table 3 Vibration values of the characteristic frequency components of horizontal measuring point

Characteristic frequency	Rigid support (m/s^2)	ISFD support (m/s^2)	Decreasing (%)
X	0.235	0.220	6.4
$2X$	0.088	0.059	33.0
X_1	0.271	0.036	86.7

Table 4 Vibration values of the characteristic frequency components of vertical measuring point

Characteristic frequency	Rigid support (m/s^2)	ISFD support (m/s^2)	Decreasing (%)
X	0.467	0.241	48.4
$2X$	0.115	0.067	41.7
X_1	0.183	0.042	77.0

Table 5 Vibration values of the characteristic frequency components of axial measuring point

Characteristic frequency	Rigid support (m/s^2)	ISFD support (m/s^2)	Decreasing (%)
X	0.090	0.072	20
X_1	0.331	0.062	81.3

References

[1] Huang X J, He L D, Wang C. Research on suppress vibration of rotor misalignment with shear viscous damper [J]. *High Technology Letters*, 2015, 21(2): 239-243

[2] Patel T H, Darpe A K. Vibration response of misaligned rotors[J]. *Journal of Sound and Vibration*, 2009, 325: 609-628

[3] Li M, Yu L. Analysis of the coupled lateral torsional vibration of a rotor-bearing system with amisaligned gear coupling[J]. *Journal of Sound and Vibration*, 2001, 243 (2): 283-300

[4] Pennacchi P, Vania A, Chatterton S. Nonlinear effects caused by coupling misalignment in rotors equipped with journal bearings[J]. *Mechanical Systems and Signal Processing*, 2012, 30: 306-322

[5] Sudhakar G N D S, Sekhar A S. Coupling misalignment in rotating machines: modeling, effects and monitoring [J]. *Noise and Vibration Worldwide*, 2009, 40(40): 17-39

[6] Ding W Q, Wu Y P, Wei W, et al. Prediction methodology research on radiant noise of aero-engine gearbox based on vibration and noise mechanism[J]. *Journal of Nanjing University of Aeronautics & Astronautics*, 2016, 48(6): 789-795 (In Chinese)

[7] Liu J Y. Study on vibration characteristics of gear system and its diagnosis method under misaligned elastic coupling [D]. Shenyang: Northeastern University, 2013. 1-5 (In Chinese)

[8] Yang S T. The research and fault diagnosis on interaction of the imbalance and misalignment in gearbox of gear shaft [J]. *Equipment Manufacturing and Education*, 2016,30 (1): 56-60

[9] Xing J, He L D, Wang K. Optimizing control for rotor vibration with magnetorheological fluid damper[J]. *Transactions of Nanjing University of Aeronautics and Astronautics*, 2014, 31(5): 538-545

[10] Memmott E A. The stability of centrifugal compressors by applications of tilt-pad seals[C]. In: Proceedings of the 8th International Conference on Vibration in Rotating Machinery, Swansea, Wales, 2004. 81-90

[11] Pietra L D, Adiletta G. The squeeze film damper over four decades of investigations. Part I: Characteristics and operating features[J]. *The Shock and Vibration Digest*, 2002, 34(1): 3-26

[12] Adiletta G, Pietra L D. The squeeze film damper over four decades of investigations. Part II: Rotordynamic analyses with rigid and flexible rotor[J]. *The Shock and Vibration Digest*, 2002, 34(2): 97-126

[13] Andrés L S, Lubell D. Imbalance response of a test rotor supported on squeeze film dampers[J]. *Journal of Engineering for Gas Turbines and Power*, 1997, 120(2): 1163-1164

[14] Ertas B, Delgado A, Moore J. Dynamic characterization of an integral squeeze film bearing support damper for a supercritical CO_2 expander [C]. In: Proceedings of ASME Turbo Expo: Turbomachinery Technical Conference and Exposition, Charlotte, USA, 2017. 1-9

[15] Ertas B, Cerny V, Kim J, et al. Stabilizing a 46 MW multi-stage utility steam turbine using integral squeeze film bearing support dampers [C]. In: Proceedings of ASME Turbo Expo: Turbomachinery Technical Conference and Exposition, Düsseldorf, Germany, 2014. 1-10

[16] Yu D D, He L D, Wan F T, et al. Suppressing vibration of rotor misalignment by means of an integral squeeze film damper (ISFD) [J]. *Journal of Beijing University of Chemical Technology* (*Natural Science*), 2018, 45(4): 65-70(In Chinese)

[17] Lu K H, He L D, Zhang Z C. Experimental study of gear shaft vibration reduction using an ISFD elastic damping support[J]. *Journal of Beijing University of Chemical Technology* (*Natural Science*), 2017, 44(1): 85-90 (In Chinese)

[18] Lu K H, He L D, Zhang Y P. Experimental study on vibration reduction characteristics of gear shafts based on ISFD installation position [J]. *Shock and Vibration*, 2017:1-10

[19] Santiago O D, Andrés L S. Imbalance response and damping force coefficients of a rotor supported on end sealed integral squeeze film dampers[C]. In: International Gas Turbine and Aeroengine Congress and Exhibition, Indianapolis, USA, 1999. 1-6

[20] Santiago O D, Andrés L S, Oliveras J. Imbalance response of a rotor supported on open-ends integral squeeze film dampers[J]. *Journal of Engineering for Gas Turbines and Power*, 1999, 121:718-724

[21] Chen P. Method research and application of roller bearing fault diagnosis based on neural network[D]. Chengdu: Sichuan University, 2006. 6-10 (In Chinese)

Lu Kaihua, born in 1991. He is studying for his Ph. D degree in Diagnosis and Self-recovery Engineering Research Center of Beijing University of Chemical Technology. He received his B. S. degree in Process Equipment and Control Engineering Department of Tianjin University of Science & Technology in 2014. His research interests are vibration control of pipeline and rotating machinery.